

Characterization of mural paintings from Cacaxtla

M. ORTEGA-AVILÉS, C. M. SAN-GERMÁN, D. MENDOZA-ANAYA
Instituto Nacional de Investigaciones Nucleares Amsterdam 46-202,
Hipódromo Condesa. 06100 México, D.F. México
E-mail: ascencio@nuclear.inin.mx

D. MORALES
Complejo Arqueológico Cacaxtla-Xochitecatl, Tlaxcala, INAH

M. JOSÉ-YACAMÁN
Instituto Nacional de Investigaciones Nucleares Amsterdam 46-202, Hipódromo Condesa.
06100 México, D.F. México; Instituto de Física, Universidad Nacional Autónoma de México,
Apdo. Postal 20-363, Delegación Alvaro Obregón, 01000 México, D.F., México

One of the most remarked customs of ancient mesoamerican cultures was that of record historical events by painting murals. It was used a rich variety of colours which is still visible in some mesoamerican buildings. In this work is reported the analysis by SEM, TEM, XRD, and FTIR, of the materials used to produce mural paintings of the archaeological zone of Cacaxtla México. The results show needle-like fibers, granular aggregates and large crystalline areas. The elemental analysis reveal a substantial concentration of O, Ca and C, followed by Si, Mg, Al, Fe, and K in lower concentration. It was found the main component in the substrate is calcite. It is also relevant the presence of palygorskite in blue and green pigments, hematite in red and pink, and calcite in white. It was also possible to identify long fibers of palygorskite on whose surface there were observed nanoparticles of metallic oxides attached. © 2001 Kluwer Academic Publishers

1. Introduction

The microstructural analysis performed in archaeological studies of pottery, paintings, stuccos and sculptures provides essential information about the origin of materials used by ancient cultures, and give information on their technological development [1–3]. In addition, archaeological materials normally suffer detriment due to environmental, biological agents and internal mechanical stresses. It is necessary to understand the physico-chemical properties of the archaeological materials, in order to avoid co-lateral effects after the application of any restoration method [3, 4].

This work presents the results obtained from several samples of mural paintings from the Cacaxtla archaeological site located in Tlaxcala, Mexico. This important site was occupied by Olmeca-Xicalanca culture during the Epiclassic period from 700 a.c. to 900 a.c. [5, 6]. Distinct cultures like Mayan, Teotihuacans and Olmecs gave a direct influence. Such influence can be observed in their buildings, pictorial representations, pottery, and sculptures.

The archaeological site of Cacaxtla has several buildings that were decorated with mural paintings, in which, war scenes, rulers and warriors such as “eagle and jaguar knights” can be observed. Several colors including red, blue, ochre, black, brown, white and green were used to perform the murals. Their principal building named The Great Basement, discovered on the 70’s, was decorated with mural paintings associated to sev-

eral architectural phases; each one elaborated with a great variety of colors [6].

Electron Microscopy Techniques have gained importance in the study and analysis of archaeological materials and art objects [7, 8]. These techniques have being used to obtain important data about colored materials [8–10]. In order to support experimental electron microscopy results, simulation studies were performed too [14, 15].

The pigments characterization was performed using different analytical techniques such as Scanning Electron Microscopy (SEM), Transmission Electron Microscopy (TEM), Fourier Transform Infrared Spectroscopy (FTIR), and X-Ray Diffraction (XRD) [12–14]. A comparison of the structural and chemical composition among different paintings is included, trying to establish the origin of the colors.

2. Experimental methods

Samples were collected directly in the archaeological site. Small fragments of paintings, each one of different color, were selected. In particular blue, red, pink, ochre, brown, white and green samples were studied. Microstructural analysis was carried out with a Scanning Electron Microscope, Phillips XL30 (SEM) fitted with an (EDAX) Energy X-ray Dispersive Spectrometer (EDS). The morphology was observed in secondary electrons mode and by mixing secondary and

backscattered electrons. The beam energy was varied from 10 to 25 KeV.

TEM analysis was performed in a Jeol-2010 microscope with a point resolution of 2.3 Å and with a Jeol 4000-EX with a maximum point resolution of 1.7 Å. Samples were prepared by removing a small fraction of the pigment from the stuccoes. This material was ground to get a fine powder. The internal structure was analyzed by using atomic resolution images.

A Siemens D-5000 X-ray diffractometer was used to identify crystalline phases. The samples were scanned from 5° to 70° in 2θ degrees, with 0.02° intervals at 30 KeV and 25 mA. Finally the identification of organic and inorganic functional groups was done by Fourier Transform Infrared Spectroscopy (FTIR) with a Nicolette Magna-IR 550 equipment, the scan was performed from 400 to 4000 cm^{-1} .

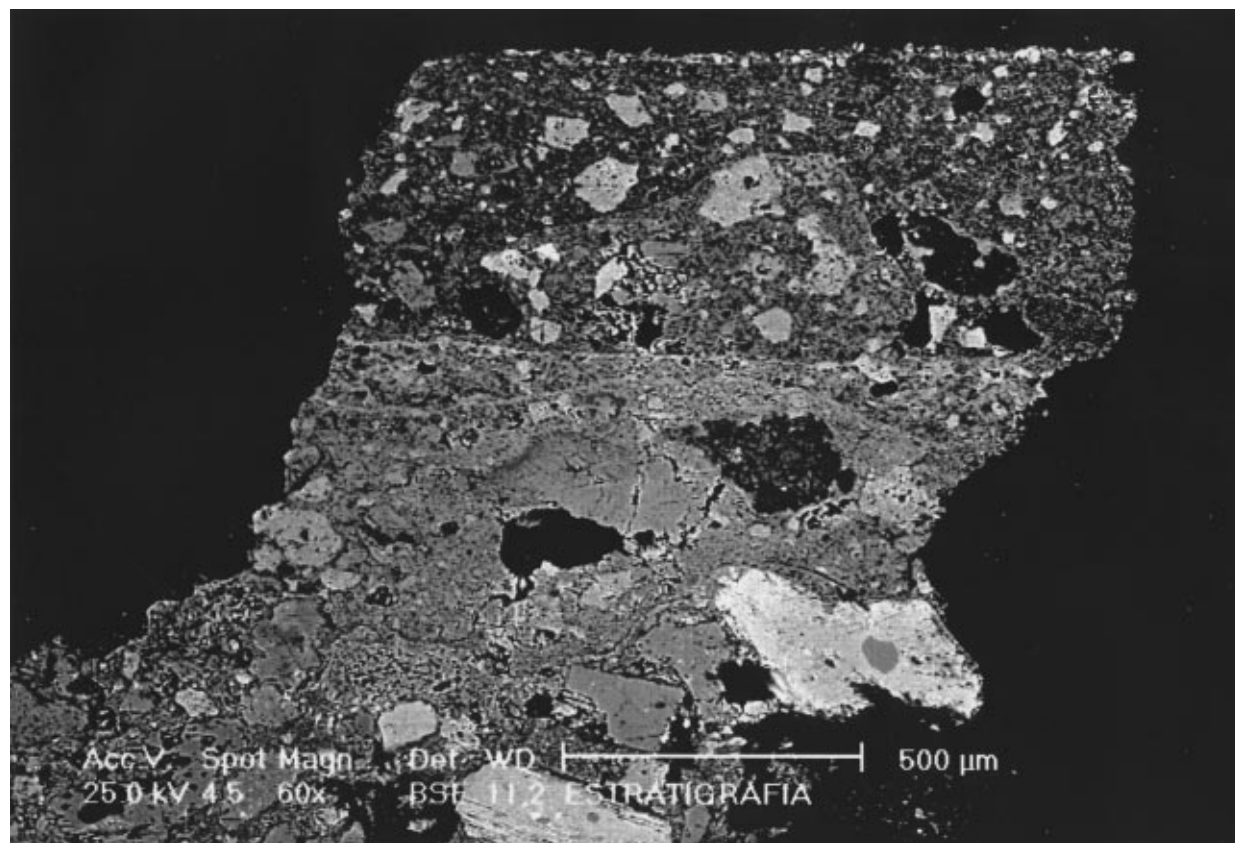
3. Experimental results

Cross sections studies of the samples showed that the thinnest paint layer is around 5–10 μm , the stucco layer is between 500 μm and 2.0 mm and the coarse plaster is near to 1.0 cm. Sometimes there is more than one paint layer in pigment samples. A general view of a sample is shown in Fig. 1a. Which corresponds to a green pigment. The grain size difference among three stratigraphic layers is evident. Some of the elements present were mapped in cross section as shown in Fig. 1b. A major concentration of Fe, Mg, Si and O was found

in the thinnest layer. Ca, C and O are distributed uniformly in the stucco layer (second layer). Particles with high silicon concentration can be seen in different areas corresponding to quartz crystals.

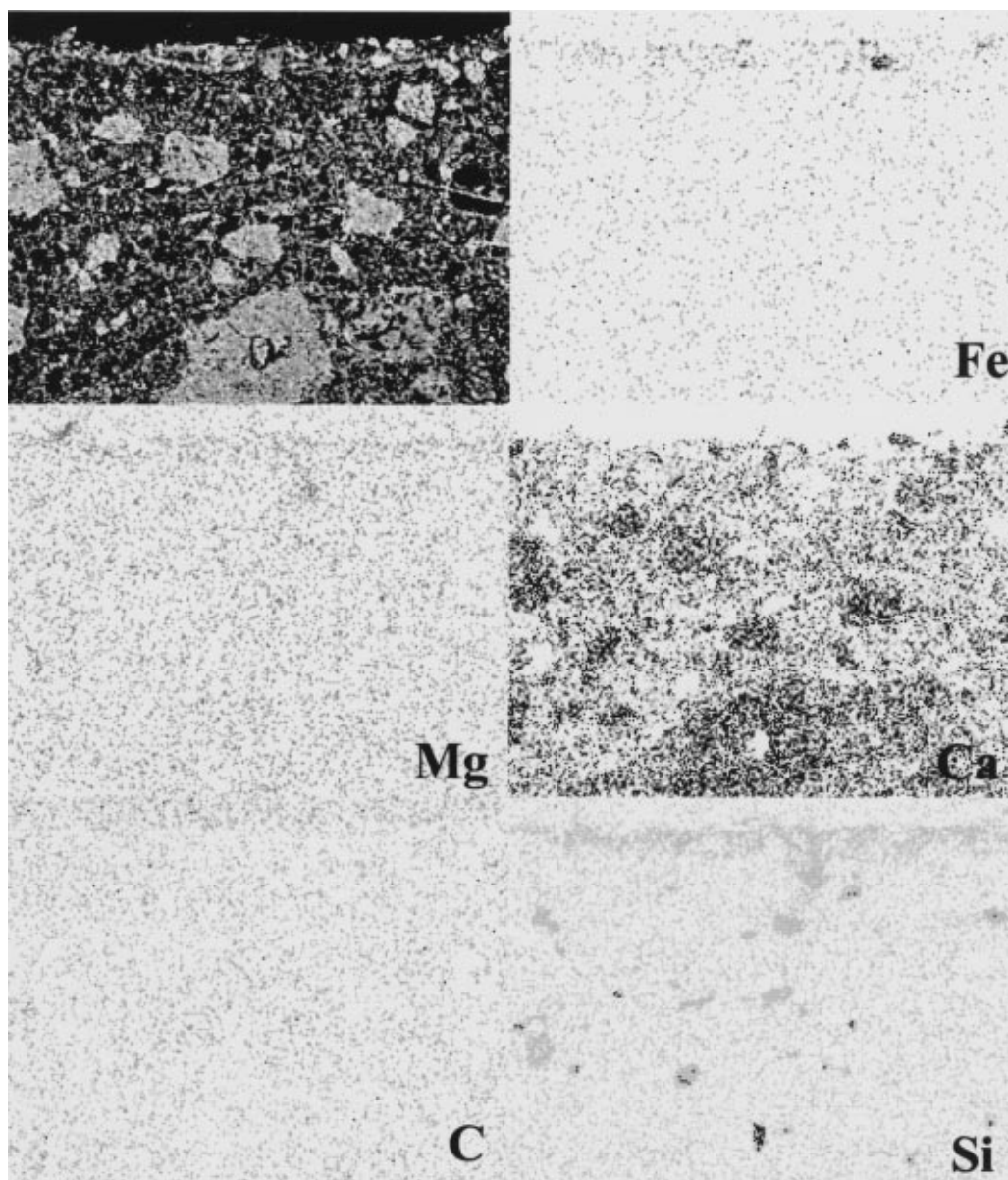
SEM analysis of **blue** pigment showed the presence of fiber-like structures. These fibers are associated to palygorskite clay [16]. In some cases, it can be observed clusters of short fibers (Fig. 2a). These fibers have a diameter range from 140 to 200 nm and 1.2 μm to 2.8 μm of length (Fig. 2b). It is possible to conclude that the artist following the direction of the fibers applied the paint. The elemental EDS analysis shows the existence mainly of O, C, Ca, Si, Al, Mg, Fe, and K. XRD spectra indicate the presence of two crystalline phases: CaCO_3 (calcite) and $(\text{Mg,Al})_2\text{Si}_4\text{O}_{10}(\text{OH})_4\text{H}_2\text{O}$ (palygorskite). High Resolution Electron Microscopy (HREM) showed the fiber lattice planes, as shown in Fig. 3. Planes correspond to the (110) palygorskite planes (10.036 Å). A few fibers correspond to sepiolite rather than palygorskite. Besides, there were observed some nanoparticles in contact with the fiber surface, which correspond to metallic oxides of Fe, Al and Sn silicates. It is remarkable that the paint contains palygorskite, which is the main component of the sakalum mineral, which comes from some regions of southern Mexico. It was used in the maya blue pigment elaboration [17, 18, 19], which is very resistant to the environmental conditions, acid concentrated solutions and bacterian action [9].

In the case of the **Red** pigment SEM images show granular aggregates sizing between 350 nm and 850 nm;



(a)

Figure 1 a) Cross section SEM image of a typical paint showing the different component plaster, stucco and pigment. b) Elemental mapping of the cross section of a typical paint; the Fe, Si, Mg, Ca, and C are observed. (Continued)



(b)

Figure 1 (Continued).

these structures are uniformly distributed. According to EDS analysis, these paintings are mainly constituted by C, O, Si, Fe, Ca, Al, Mg, and K. The red pigments showed an important amount of iron $\sim 19\%$ (atomic percent). XRD analysis showed that $\alpha\text{-Fe}_2\text{O}_3$ (hematite) was the main crystalline phase in the red pigment. Calcite was present in the stucco. Opaque iron nanoparticles were found by TEM (Fig. 4). EDS analysis indicate the presence of Fe and O and minor amounts of C, Si and Al. The atomic ratio between Fe and O, which is 2 : 3, confirms that this particle correspond to the hematite crystalline phase ($\alpha\text{-Fe}_2\text{O}_3$). This phase is a very stable mineral obtained from dehydration of hydrated iron oxides such as limonite (hydrated Fe oxides), lepidocrocite ($\text{FeO}(\text{OH})$), and goethite ($\text{FeO}(\text{OH})$).

A physical mixture of $\alpha\text{-Fe}_2\text{O}_3$ and CaCO_3 was found in the **pink** pigment. SEM images agglomerates of $\alpha\text{-Fe}_2\text{O}_3$, CaCO_3 , and quartz crystals. By EDS, it was possible the identification of a low percentage of

Sr, which also could contribute to this color, as a component of CaCO_3 . This hypothesis agrees with XRD results. A typical electron micrograph of this paint can be seen in Fig. 5.

The **ochre** painting morphology is characterized by a compact surface constituted by flake-like particles of 5 to 20 μm and massive granular particles. Two distinct kinds of agglomerates were found; the first one is around 16 μm in diameter formed by particles of 600 nm approximately (Fig. 6a). The second ones are compact agglomerates in a range size from 30 nm to 3 μm . The sample presents small areas with fiber like structures, similar to the observed in the blue paint layer. The observed fibers in the ochre paint correspond to a blue paint layer, and the ochre paint was applied over the blue paint layer. We found long fibers, grouped in bundles of 3 μm to 5 μm in length (Fig. 6b). The elemental composition in ochre painting is mainly conformed by C, O, Si, Ca and Fe; however, Al, and Mg were

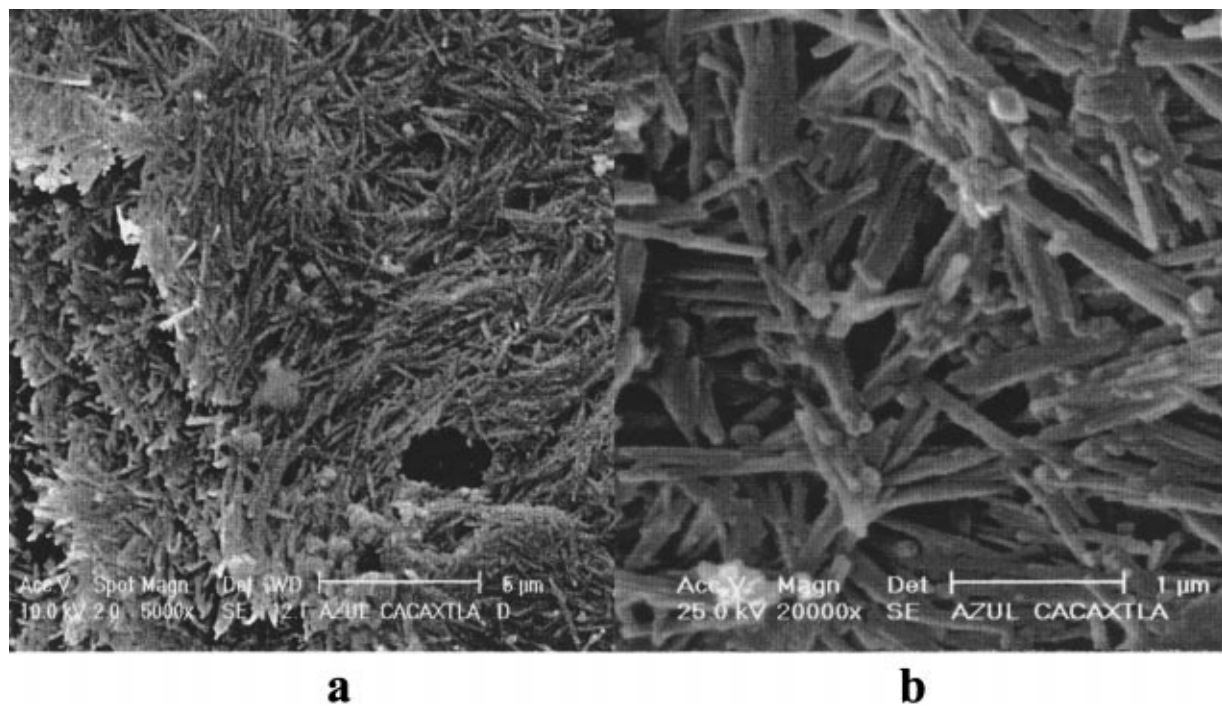


Figure 2 SEM images from palygorskite fibers observed in blue pigments, a) section shows short size clustered fiber. b) Section showing clustered fibers.

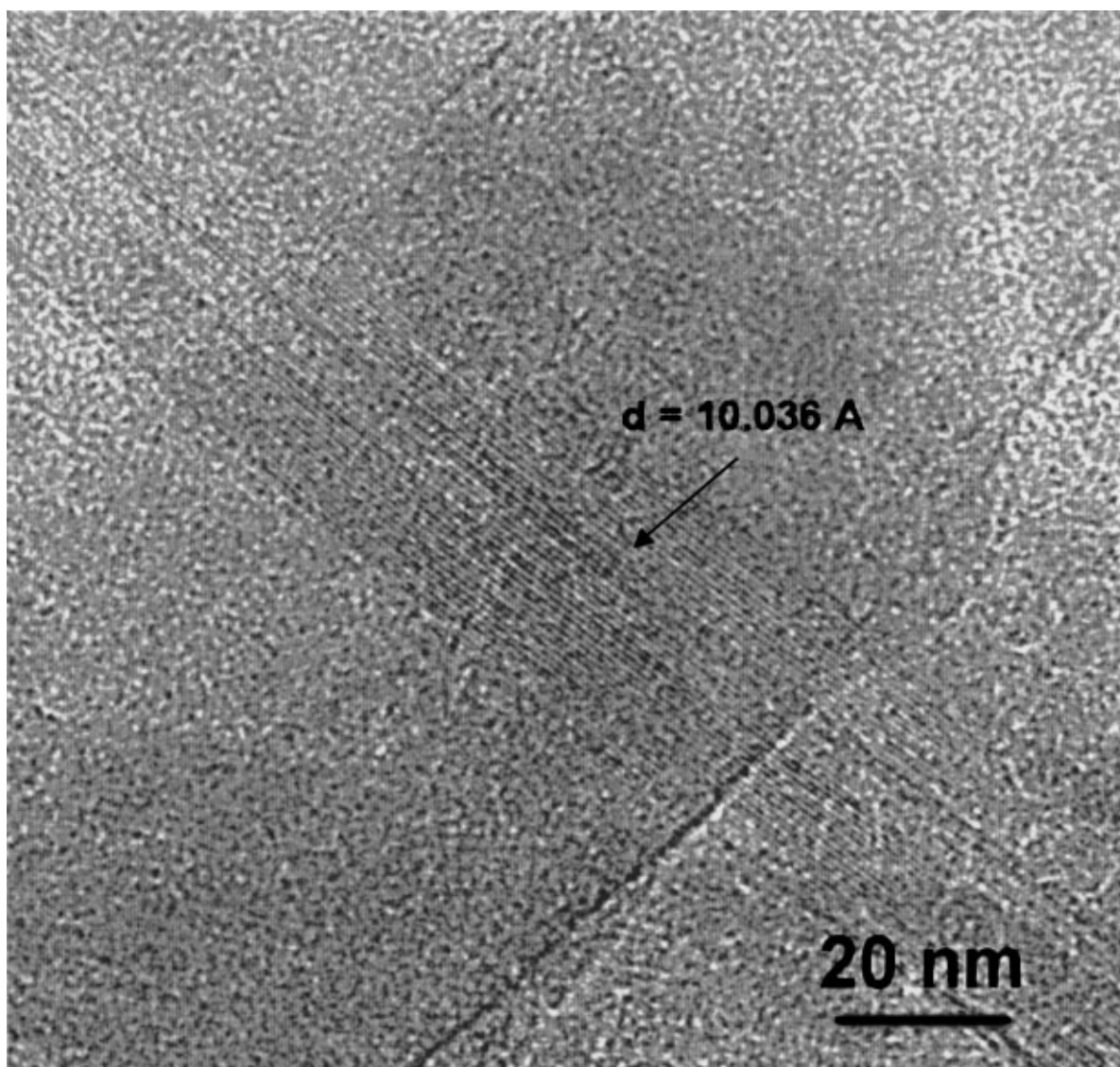


Figure 3 High Resolution TEM image of a palygorskite fiber which also contains a $\alpha\text{-Fe}_2\text{O}_3$ particle. The fiber shows a $d = 10.036 \text{ \AA}$ interplanar distance corresponding to (1 1 0) planes of palygorskite.

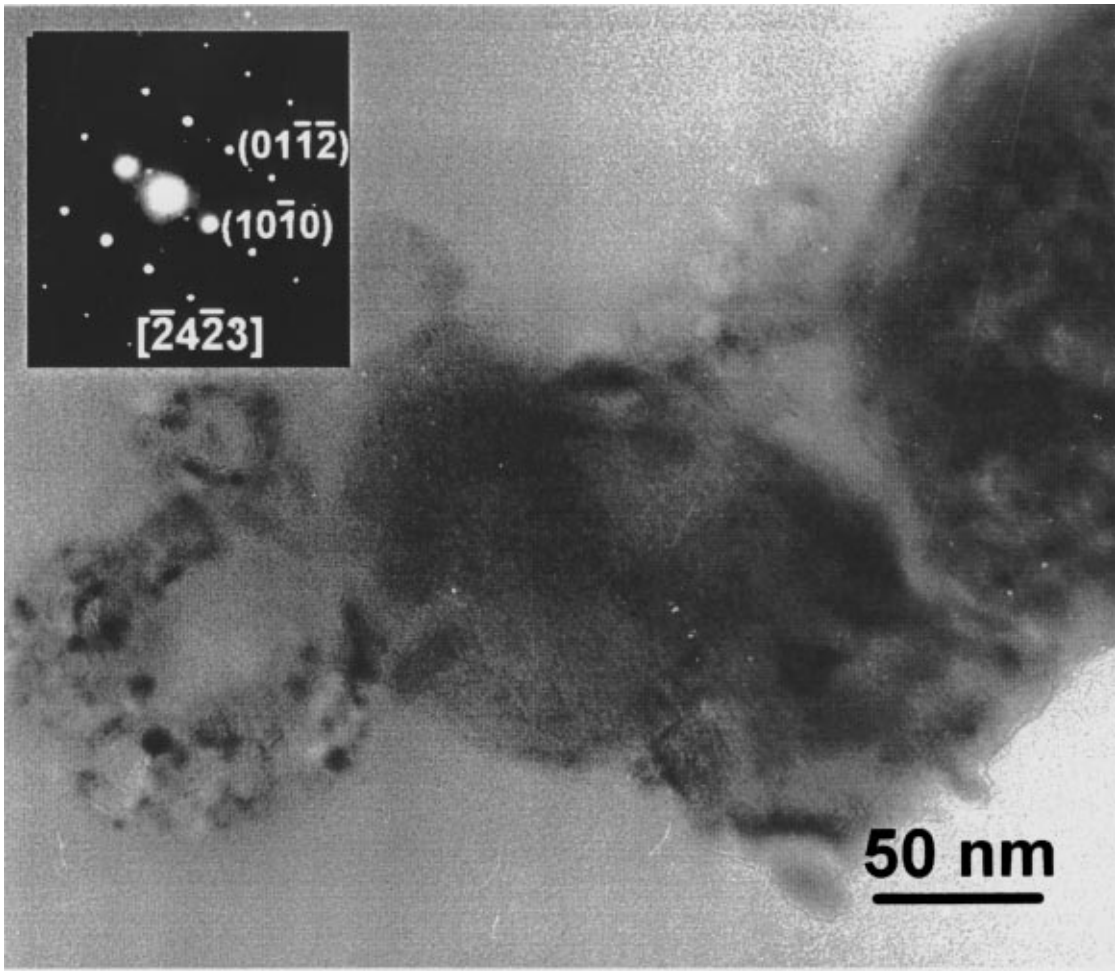


Figure 4 Bright field TEM image the inset shows the electron diffraction pattern of $\alpha\text{-Fe}_2\text{O}_3$ (hematite). The zone axis is $(\bar{2}4\bar{2}3)$.

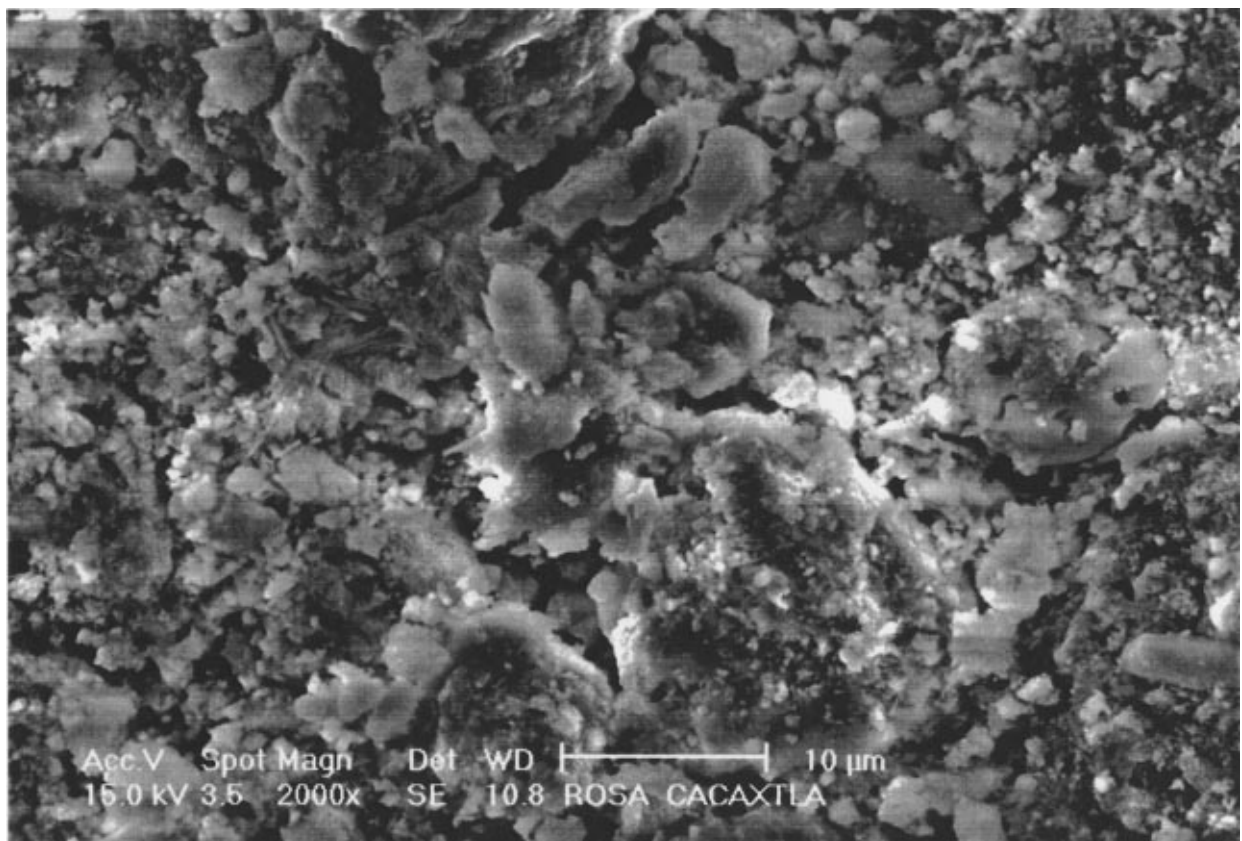


Figure 5 SEM image from pink pigment shows hematite crystals and agglomerates from calcite, which form this pigment.

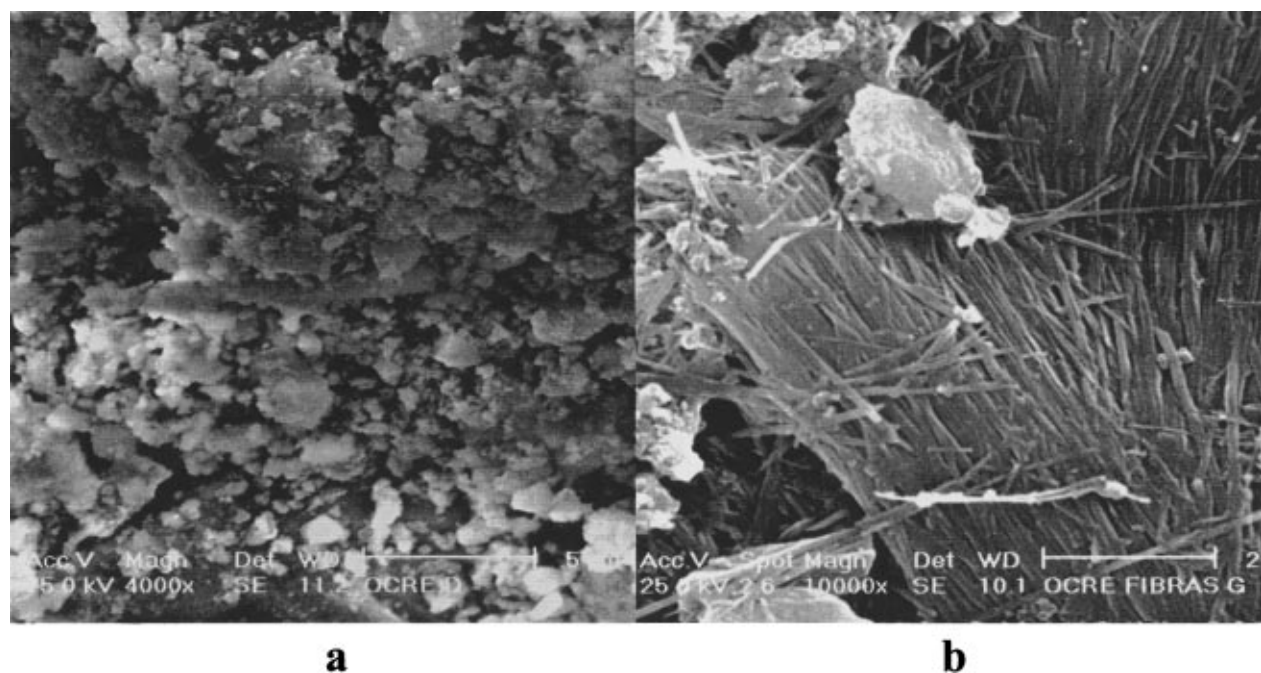


Figure 6 SEM image from ochre pigment. a) Agglomerates of calcite. b) Fibers of palygorskite forming bundles.

also identified in fewer proportions. In this pigment, we also found the crystalline phases CaCO_3 , SiO_2 , $\text{CaMg}(\text{CO}_3)_2$ and $\text{NaAlSi}_3\text{O}_8$. There were identified nanoparticles with high concentration of Ca and some silicates by electron diffraction in TEM. Bands in the infrared spectrum corresponding to calcite, quartz and H_2O molecules were identified by FTIR (Fig. 7). It was also possible to appreciate some bands associated to organic compounds, such as the band at 1798 cm^{-1} which corresponds to aromatic rings; the bands at 2920 cm^{-1} and 2852 cm^{-1} belong to CH_2 groups; it is interesting to notice that the absorption band at 1728 cm^{-1} which corresponds to $\text{C}=\text{O}$ bond, appears only in the ochre pigment.

Needle-like fibers were observed in **Green** pigment with diameters smaller than 150 nm and $3\text{ }\mu\text{m}$ of length, very similar to those observed in the blue painting (Fig. 8a). Moreover, it was observed agglomerates of particles with in a diameter range of 200 nm to 600 nm , which are distributed uniformly above the entire surface (Fig. 8b). In all cases it can be observed agglomerates of fibers with a diameter of $30\text{ }\mu\text{m}$ approximately, forming a large grain. According to the EDS analysis, those agglomerates of particles present O, Ca, C, and in lesser proportion Si; in the fibers area C, O, Si, Ca, Mg, Al, Fe, and K were identified. In this particular case, it was not possible to use other characterization techniques, due to the small amount of sample (this color was the less frequently used).

Brown pigment morphology is constituted mainly by a large amount of granular particles with a size $\sim 170\text{ nm}$, these particles form aggregates of $1.2\text{ }\mu\text{m}$ in diameter as shown in Fig. 9. All these particles are supported on a flat surface. Elements like C, O, Ca, Si, Al, Mg, Fe, K, and P were identified by EDS analysis as main components. Calcite (CaCO_3), quartz (SiO_2), dolomite ($\text{CaMg}(\text{CO}_3)_2$), and albite ($\text{NaAlSi}_3\text{O}_8$) are

the crystalline phases present in the brown pigment. It is important to mention that all these compounds could turn into a brownish color by the presence of impurities or by cationic exchange [9]. The infrared spectrum is shown in Fig. 7, could be identified typical bands corresponding to calcite, quartz and H_2O molecules. Some bands are associated to organic compounds, as the band at 1798 cm^{-1} corresponding to aromatic compounds, bands at 2920 cm^{-1} and 2852 cm^{-1} belong to CH_2 groups, also we could observe that the infrared spectrums of white and ochre pigments are very similar, a small difference in bands intensity is observable and we can observe a little shift towards a short wave numbers respect to ochre spectrum.

White pigment shows a morphology of compact agglomerates made by granular particles (Fig. 10), EDS analysis shows large amounts of Ca, C, and O. XRD analysis showed the CaCO_3 , SiO_2 and $\text{NaAlSi}_3\text{O}_8$ as crystalline phases. FTIR presents typical bands corresponding to CO_3 groups, Si-O bonds and H_2O molecules were identified. It was possible to appreciate some bands associated to organic compounds, like the band at 1798 cm^{-1} belonging to aromatic overtones, 2920 cm^{-1} and 2852 cm^{-1} correspond to CH_2 groups as shown in Fig. 7. In Fig. 11, we report the observed variation in atomic percent of some typical elements (Mg, Al, Si, Ca, Fe) from minerals, found in different samples.

In Table I we present a summary of the elemental composition in atomic percent of the analyzed paintings, while Table II is a summary of the crystalline phases identified in the samples. Furthermore, it is interesting to notice the presence of the needle-like fibers associated to palygorskite clay in other pigments, such as green and ochre. In a previous work [19] about Maya paintings, it was reported that the palygorskite

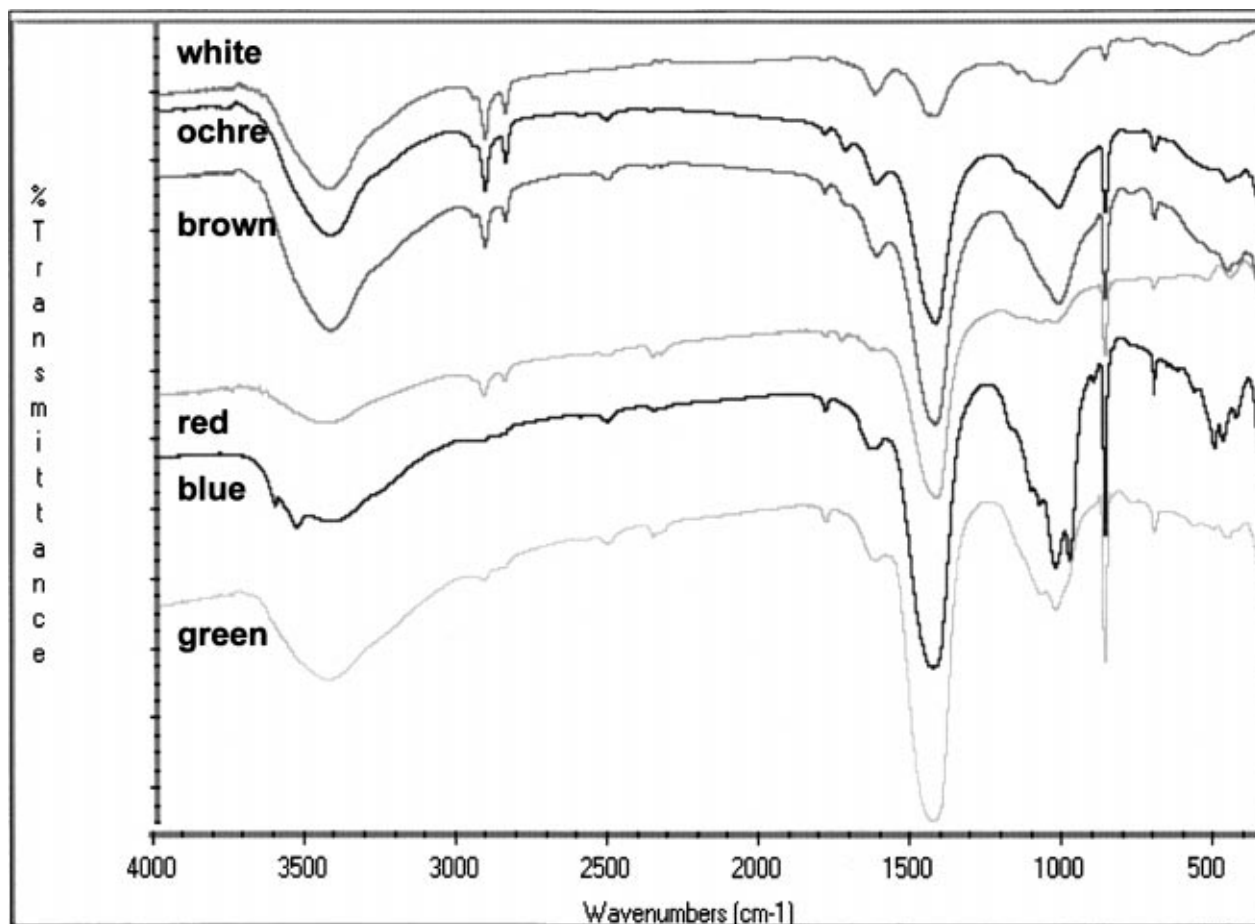


Figure 7 FTIR spectra of ochre, brown and white pigments, show characteristic bands from calcite, C=O groups, CH₂ groups and overtones from aromatic compounds.

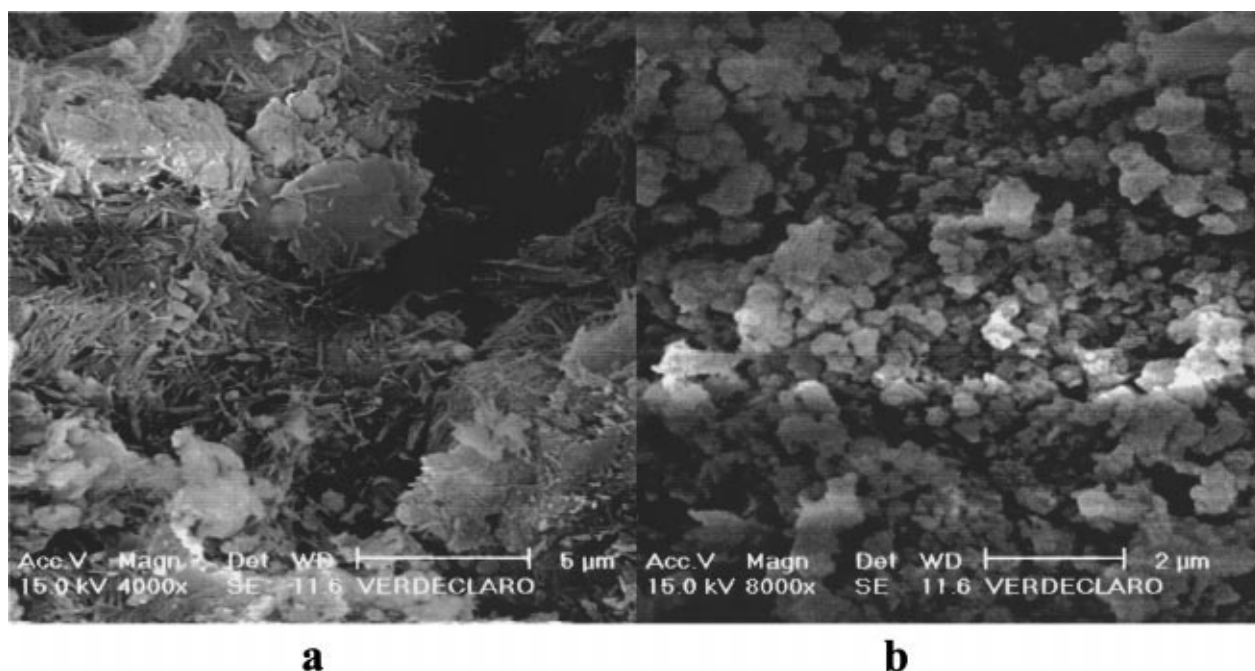


Figure 8 Micrograph of green paint, a) region containing fibers in non agglomerated state. b) Region shown agglomerates of little crystals.

fibers were found in blue pigments. In the present work we found that this colorant is also observed in green and ochre pigments. Palygorskite was also found in the green pigment from Maya sites, but not in the ochre, and this is because used samples of ochre pigment came

from a mural (known as The warriors battle) which had a previous layer of blue pigment. Therefore, it is possible that the palygorskite fibers observed in the sample were the result of contamination from the blue layer.

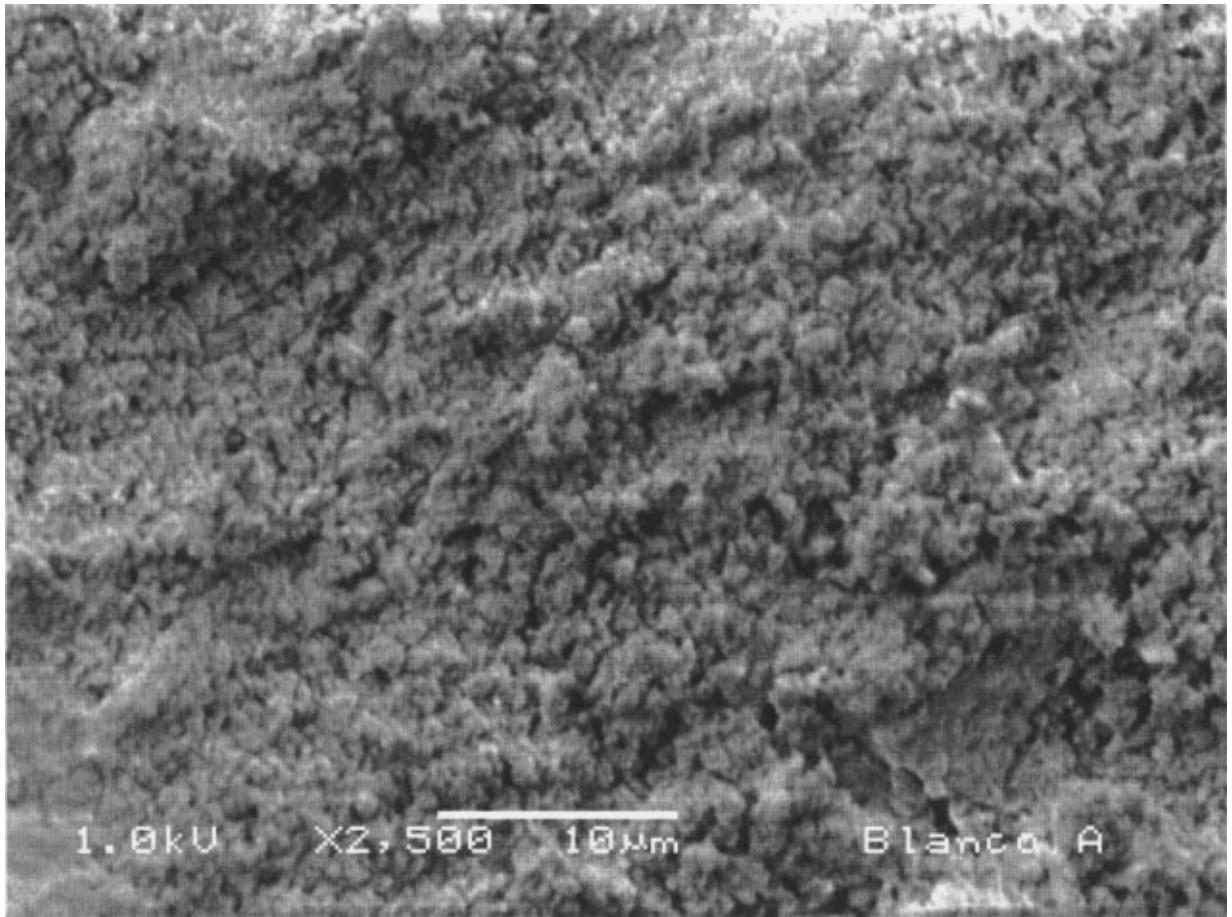


Figure 9 Low vacuum SEM image from brown pigment, we can observe agglomerates with porous appearance, similar to calcite in ochre and white pigments.

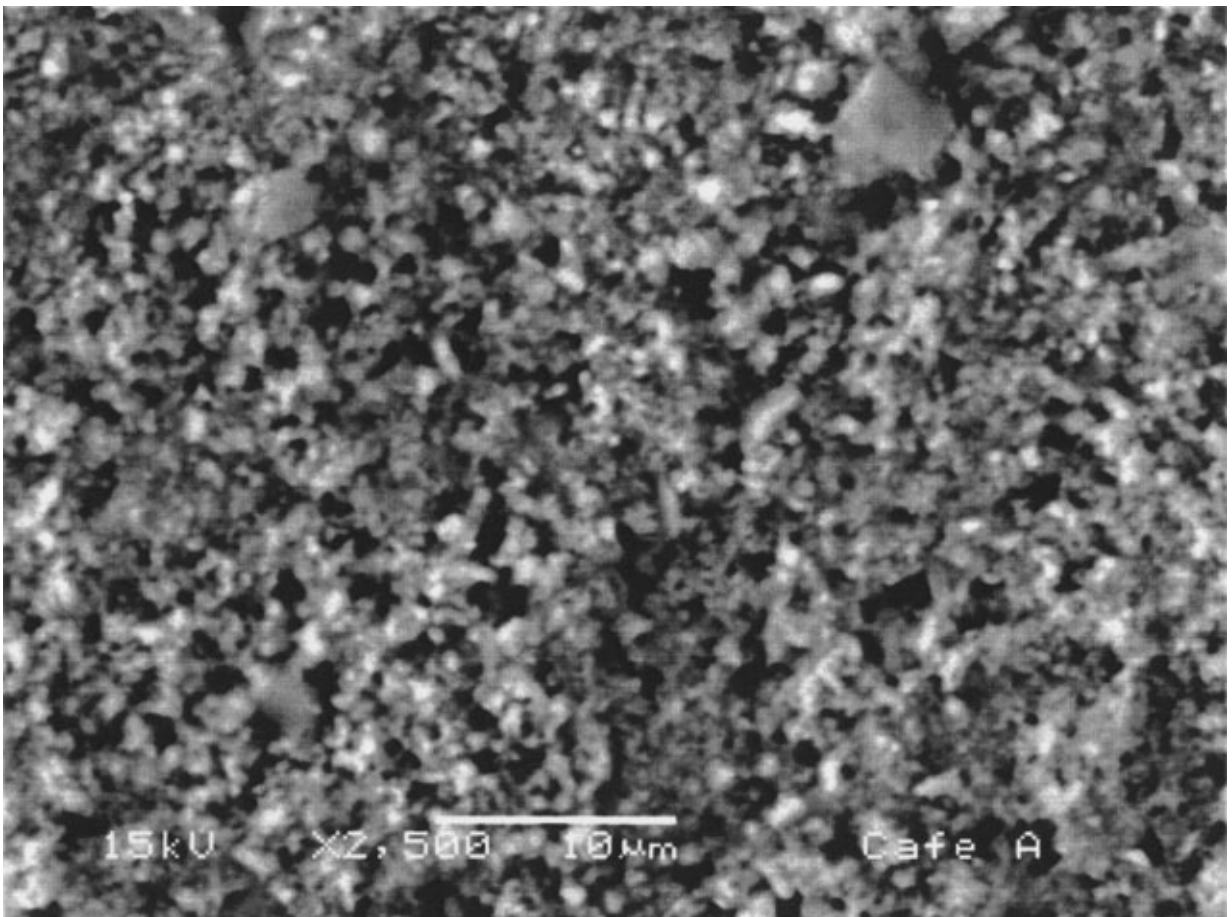


Figure 10 Low vacuum SEM micrograph from white pigment constituted by calcite mainly.

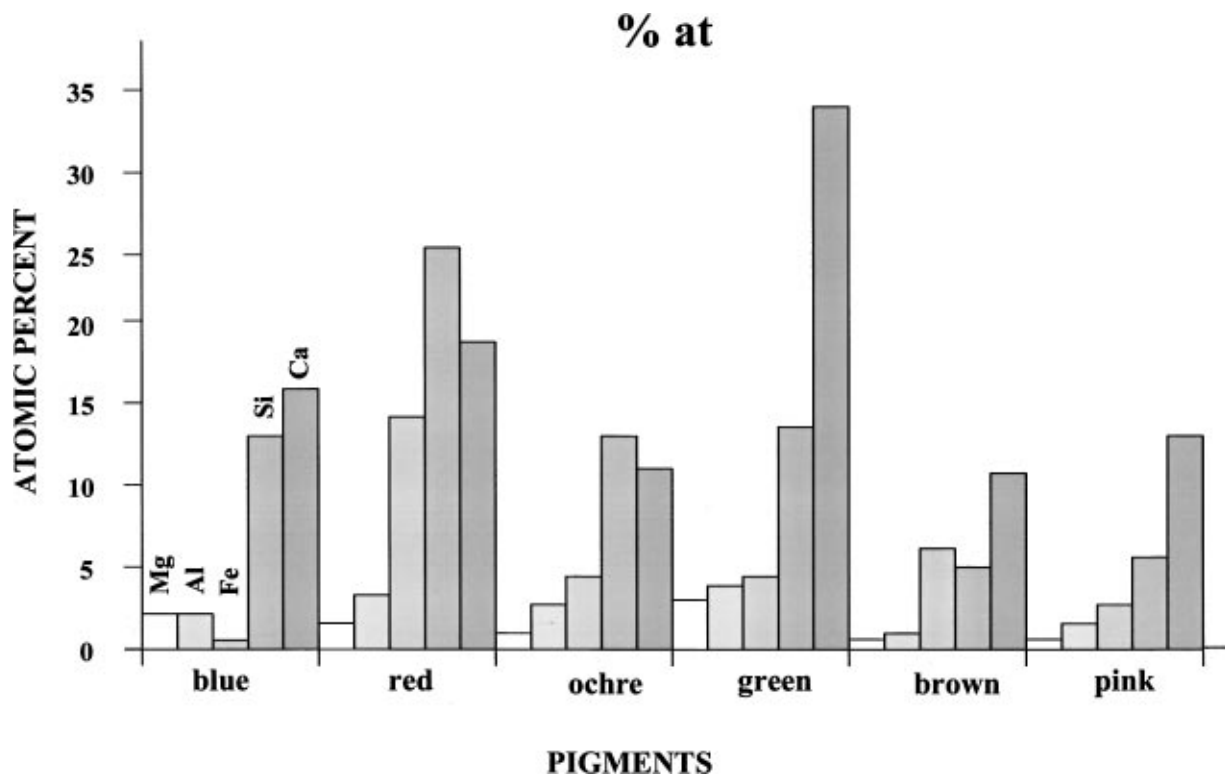


Figure 11 Variation on the atomic percent of some elements identified in the samples of different color.

4. Discussion and conclusions

According to the SEM and TEM results, fibrous and granular shapes with nanometric size are the dominant structures in the blue paintings, while granular agglomerates are present in red, pink, brown, white, and ochre paintings. CaCO_3 , SiO_2 , $\text{NaAlSi}_3\text{O}_8$ and $(\text{Ca}, \text{Na})(\text{Si}, \text{Al})_4\text{O}_8$ are the main components of the samples that could be associated to the substrates or stuccoes; other crystalline phases such as $(\text{Mg}_8(\text{H}_2\text{O})_4(\text{OH})_4\text{Si}_{12}\text{O}_{30})$, $\alpha\text{Fe}_2\text{O}_3$ and $\text{CaMg}(\text{CO}_3)_2$ were identified, the last mineral is associated to palygorskite growths in nature. Palygorskite was also associated to blue and green pigments, while hematite was associated to red pigment. Dolomite, calcite, and albite were associated with ochre painting.

Atomic percent variation of some elements showed that Mg, and Al have a linear tendency as it can be observed in Fig. 11; their percentage is between 0.5 and 3% (atomic percent). Green and blue pigments have the highest amounts of Mg and Al, due to the palygorskite structure (octahedral site). Red pigment contains the largest percentage of Fe, followed by the brown, ochre, green, pink, and blue pigments. Silicon has a similar tendency as the iron variation, except for the brown pigment, and all the samples contain around of 15% (atomic percent) of Ca. The lowest amount of calcium was found in ochre and brown pigments.

Calcite was used as a substrate for the pigments, this is an indicative of the painting technique used, in this case it was fresco or a mixed technique of fresco and tempera. Calcite mineral was used to have better adhesion between the pigment and the substrate. A curious fact is that plaster has a high alkali concentration, which has a tendency to bleach out pigments. However, the mineral pigments identified in the samples

do not bleach out in fresco technique. XRD results indicate that the plaster was made using feldspars rich in Sodium, calcite and quartz. HREM results of ochre pigments indicate that the main particles are rich in calcium, in its carbonate form. It was possible to identify opaque particles of iron oxide in the red pigment and calcium particles too. The metallic nanoparticles play an important roll in the materials color, some of these particles such as iron and aluminum oxides could be identified and characterized by HREM. On the other hand, traces of elements identified by EDS, such as Barium in the structure of calcite could be turned to pink, and iron could be turned to yellow or brown according to the literature. These elements are in the crystalline structure by cationic exchange with other minerals.

FTIR analysis provides evidence of organic compounds in the paintings. In the range of $1500\text{--}2700\text{ cm}^{-1}$ of the IR spectrum, there are not characteristic bands from minerals. Therefore, bands which correspond to organic functional groups, such as 1798 cm^{-1} band (aromatic compounds); 2920 cm^{-1} and 2852 cm^{-1} (CH_2 groups); absorption band at 1728 cm^{-1} which belongs to $\text{C}=\text{O}$ bond. The last one appears only in the ochre pigment, and all these bands must belong to vegetable gums used as binder in pigment applications over the wall.

The Olmeca-Xicalanca culture used a technique for elaborating their wall paintings similar to the Maya technique. The blue pigment is like the maya blue paint used by the Maya culture and the green pigment is also like the maya green, which was elaborated using palygorskite may be maya blue combined with any ochre pigment to obtain green color. This last pigment is a physical mixture of two pigments: blue and ochre. SEM confirmed this fact.

Colorant materials are basically minerals with the exception of the blue paint, which is a combination of a palygorskite matrix and indigo dye, in maya blue FTIR spectrum was possible to identify characteristic bands of the mineral clay palygorskite. A curious fact is that was not possible to separate the indigo dye and the clay as was claimed by Cabrera [19]. To our knowledge no other group has also reproduced the Cabrera Claim.

It should be concluded that the technology used by the Olmeca-Xicalanca culture in their paintings was totally equivalent to the Maya culture. This suggests a very strong contact between these two cultures. In fact the dating of the paints suggest that the maya blue was developed in a larger region of Mesoamerica. Therefore, the original description of the blue colorant as maya blue might not be totally correct.

Acknowledgements

The authors are indebted to L. Rendón, S. Tehuacanero and T. Santamaria for technical support. This work was supported by CONACYT through the grant "Coloides Cuánticos," puntos cuánticos y nanopartículas. We thank The "Consejo de Arqueología del INAH" for permission to the study of pigments from Cacaxtla archaeological site.

References

1. R. GIOVANOLI, *Archaeometry* **11** (1969) 53.
2. K. D. MAGALONI, M. AGUILAR and V. CASTAÑO, *Proceedings of the Material Research Society Symposium* **185** (1991) 145.
3. M. JOSÉ-YACAMÁN and J. A. ASCENCIO, "Modern Methods In Art And Archeology" (John Wiley and Sons, 1999).
4. M. A. FERRER, "La pintura mural, su soporte, conservación, restauración y las técnicas modernas" (Universidad de Sevilla, 1995).

5. M. FONCERRADA DE MOLINA, "Cacaxtla La Iconografía de los Olmeca-Xicalanca" (UNAM, 1983).
6. K. D. MAGALONI, "Metodología para el análisis de la técnica pictórica mural prehispánica: El templo rojo de Cacaxtla" (Colección científica INAH, 1994).
7. M. S. TITE, "Methods of Physical Examination in Archaeology" (Seminar Press, London and New York, 1972).
8. M. JOSÉ-YACAMÁN, L. RENDÓN, J. ARENAS and M. C. SERRA PUCHE, *Science* **273** (1996) 223.
9. D. MENDOZA-ANAYA, V. RODRÍGUEZ-LUGO, G. MARTÍNEZ-CORNEJO and M. JOSÉ-YACAMAN, in *Proceedings of the ICEM 14* (Cancun, Mexico, 1998) Vol. 3, p. 253.
10. V. RODRÍGUEZ-LUGO, L. ORTÍZ-VELÁZQUEZ, J. MIRANDA, M. ORTÍZ-ROJAS and V. M. CASTAÑO, *Journal of Radionuclital and Nuclear Chemistry* **240** (1999) No. 2.
11. M. J. WILSON, "Clay Mineralogy" (Chapman & Hall, 1980).
12. P. K. HAROLD and L. E. ALEXANDER, "X-Ray Diffraction Procedures for Polycrystalline and Amorphous Materials" (John Wiley and Sons, 1974).
13. D. M. MOORE and R. C. REYNOLDS, JR., "X-Ray Diffraction and the Identification and Analysis of Clay Minerals" (Oxford University Press, 1997).
14. M. MENDOZA SERRANO, Master Thesis, "Procesamiento digital de Imagnes y vision aplicado a materiales nanoestructurados" (ININ-ITT, 1999).
15. M. ORTEGA, J. A. ASCENCIO, C. M. SAN-GERMAN, M. E. FERNANDEZ, L. LOPEZ-LUJAN and M. JOSE-YACAMAN, *J. Mater. Sci.*, in press.
16. M. E. FERNÁNDEZ, J. A. ASCENCIO, D. MENDOZA-ANAYA, D. V. RODRÍGUEZ-LUGO and M. JOSÉ-YACAMÁN, *ibid.* (1999).
17. M. JOSÉ-YACAMÁN, L. RENDÓN and M. C. SERRA PUCHE, in *Proceedings of the Material Research Society Symposium* (1995) Vol. 352, p. 3.
18. L. TORRES-MONTES, in *Proceedings of the Material Research Society Symposium* (1998) Vol. 123, p. 123.
19. J. M. CABRERA GARRIDO, "Informes y Trabajos del Instituto de Conservación y Restauración de Obras de Arte, Arqueología y Etnología" (Artes Gráficas Soler, 1969) Vol. 8, p. 1.

*Received 11 April
and accepted 15 September 2000*